

## Porous cellulose propionate induced by mobile phase for specific channels

Jisoo Lee and Sang Wook Kang<sup>†</sup>

Department of Chemistry and Energy Engineering, Sangmyung University, Seoul 03016, Korea

(Received 18 May 2023 • Revised 19 June 2023 • Accepted 18 July 2023)

**Abstract**—A polymer with pores close to a straight line was prepared by adding a plasticizer lactic acid to cellulose propionate. We succeeded in preparing for the porous cellulose propionate (CP) by a low-cost and eco-friendly manufacturing process with water treatment technology. The CP used in this study has a higher molecular weight and better mechanical strength than the cellulose acetate (CA) widely used for the membrane. In general, as the molecular weight of the polymer increases, the mechanical strength can be stronger. Thus, porous CP can be manufactured as a single film without additional polymer support. The additive LA can penetrate into the CP chains and plasticize the membrane to form pores. The manufactured membrane was installed in a water treatment machine and hydraulic pressure was applied from 2 to 7 bar. The surface and the cross-section of the membrane were verified using SEM, and the membrane, to which hydraulic pressure was applied with a plasticizer, showed a surface in which pores were generated. Then, FT-IR was investigated to confirm how the interaction between the functional groups between CP and LA changed.

Keywords: Cellulose Propionate, Lactic Acid, Channel, Porosity

### INTRODUCTION

The supply of electric vehicles has been increased worldwide [1-3], and the use of an energy storage system (ESS), a device that can store new and renewable energy such as solar and wind power in advance and use it at the necessary time, is increasing [4,5]. Additionally, as 'Codeless' industrial products such as the Internet of Things (IoT) and wireless home appliances have been commercialized, the importance of the battery industry is becoming more emphasized [6-9]. Among them, as demand for small portable electronic devices such as mobile phones and laptops increases, lithium ion batteries having a smaller size and a faster charging speed are required. As electronic devices become smaller, the battery becomes smaller, and the distance between the cathode and anode becomes shorter [10,11]. As the demand for miniaturized electronic devices increases, thinner separators have been used to reduce the size of batteries and enhance the efficiency. As a result, as the separator thickness becomes thinner, stability problems such as the risk of battery explosion are emerging. Eventually, several fire accidents have occurred where the separator could not withstand heat and exploded. Thus, interest in battery stability has exploded recently [12,13]. The separator is made of a porous structural membrane so that ions can pass through it, which has the property of having mechanical strength [14,15]. Methods of manufacturing separators are largely divided: (1) a dry method of manufacturing pores by pulling the film horizontally or vertically, and (2) a wet method of generating holes in the membrane by adding a plasticizer to polymer. Although the dry method is inexpensive since the manufacturing process is simple, however, the size of pores is not uniform due to the forma-

tion of holes by a mechanical force. A wet method, commonly used in electric vehicle batteries, creates pores through chemical methods; thus, it has stronger mechanical strength and could make the pore size uniform, resulting in that lithium ions could move more efficiently. Although the manufacturing process of wet method is more complicated than the dry method, it can be made thinner, and its energy density is greater. Separator materials to prevent cathode and anode contact contribute greatly to battery stability. When manufacturing separators, existing methods such as phase separation can be used to produce irregular and random holes. It requires the shortest path when  $\text{Li}^+$  ions pass through the separator [16,17]. As the charging speed takes longer if the movement path of  $\text{Li}^+$  ions increases, it is recommended to generate a hole straight in the separator to speed up the charging speed. The track etching method [18], which uses radiation [19], allows the separator to make holes in a straight line, but it is expensive to commercialize.

Furthermore, lithium-ion batteries used in electric vehicles are considered as waste when their performance drops to about 7-80%. As the demand for batteries increases due to the spread of electric vehicles and electronic devices, the problem of waste batteries is also being raised. As a result, environmental problems caused by waste batteries are emerging as important [20,21]. This experiment uses cellulose-based materials extracted from plants, and thus it is possible to manufacture eco-friendly battery separators. Our group recently proposed a method of making holes close to a straight line using a hydraulic process. This method is simple and relatively inexpensive. In addition, it is easy to recycle and is eco-friendly. In our laboratory, cellulose acetate (CA) was used to make membranes, and it was confirmed that the charging speed in battery cell performance increased and the thermal stability improved [22-27]. Therefore, it is generally coated on a support such as polypropylene (PP), but applying this method requires a considerable of additional process. Since an additional process is not required when manufac-

<sup>†</sup>To whom correspondence should be addressed.

E-mail: swkang@smu.ac.kr

Copyright by The Korean Institute of Chemical Engineers.

tured with a single film, we suggested cellulose propionate (CP) as a new matrix among the inexpensive cellulose derivatives with better mechanical properties. Thus, CP based on cellulose is presented as a single separator film for the first time, which has a higher molecular weight and better mechanical properties than CA. In particular, it is expected that by applying water treatment on CP, it is possible to control the porosity of the membrane to an appropriate size. Lactic acid (LA) is used as a plasticizer since it is a hydrophilic material capable of mixing easily with a solvent and is inexpensive. If CP

polymer and the suggested method are all used, the membrane can be made as a single film, and it would be more economical in the process and eco-friendly since cellulose polymers are used.

### EXPERIMENTAL

Cellulose propionate (Mn ~70,000, Sigma-Aldrich Chemical Co.), and lactic acid (Daejung Chemical & Metals) were utilized as the membrane materials. Dimethylacetamide (Sigma-Aldrich) and etha-

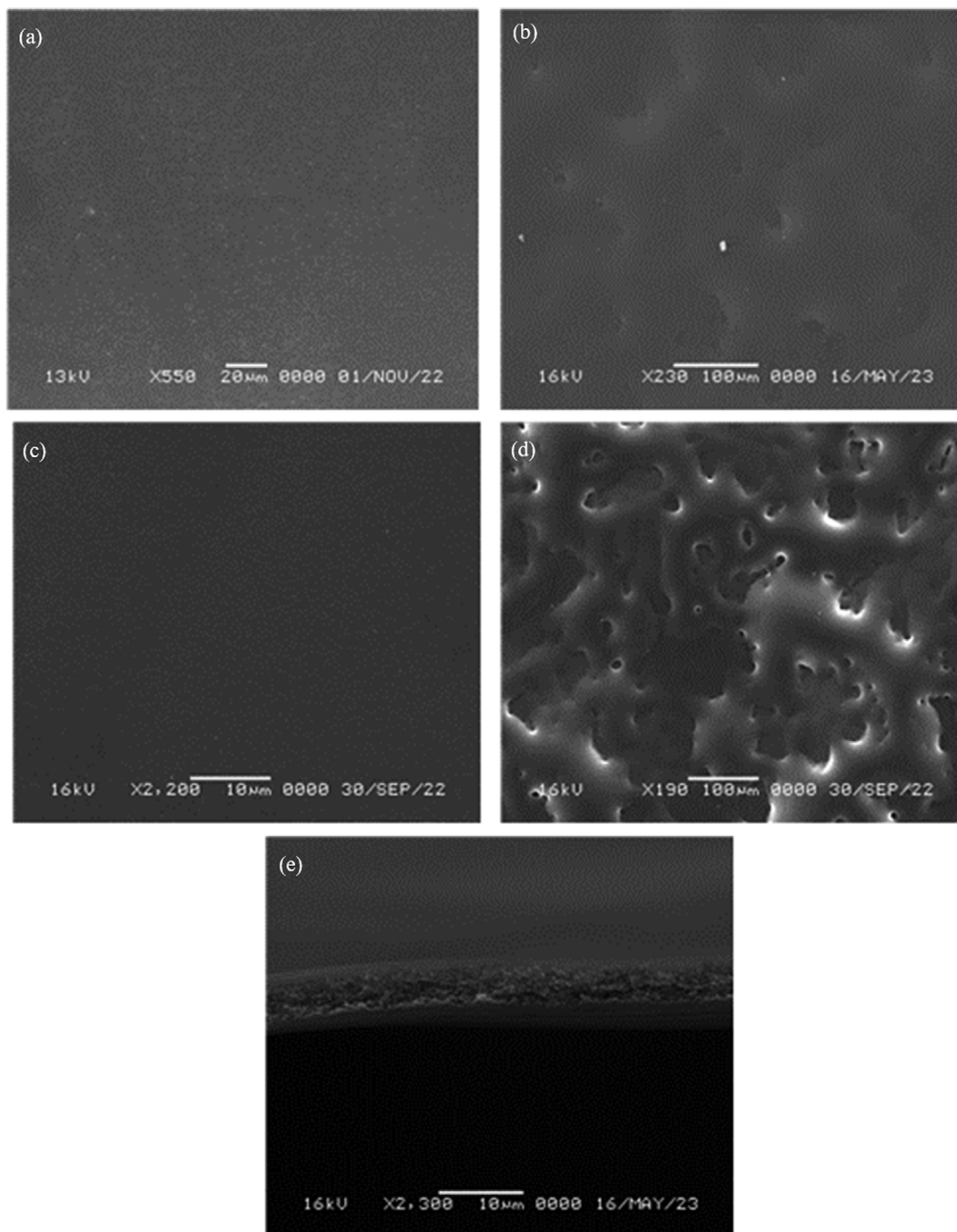


Fig. 1. (a) neat CP dissolved in DMAc/EtOH (8:2), (b) neat CP at 7 bar, (c) CP with LA (1:0.05) dissolved in DMAc/EtOH (8:2) at 0 bar, (d) CP with LA (1:0.05) dissolved in DMAc/EtOH (8:2) at 7 bar, (e) cross-section of CP with LA (1:0.05) dissolved in DMAc/EtOH (8:2) at 7 bar.

nol (Daejung Chemical & Metals) were used as the solvent.

Cellulose propionate (Mn ~70,000) was put into the dimethylacetamide (DMAc)/ethanol (8:2) to make a 3 wt% neat CP membrane. (CP: 0.3 g, DMAc: 7.702 g, EtOH: 1.928 g, LA: 0.011 g) 0.05 mol ratio of lactic acid used as plasticizer to make pores easily. The solution was stirred for about 24 hours. Then, a doctor blade was put on the edge of a clean glass plate and utilized as coating method. The glass plate with the solution was put in a 70 °C oven for 30 minutes and moved to a thermostat with a temperature of 25 °C and a humidity of 50% to dry it for 30 minutes. Then, the manufactured membrane was cut into three pieces and installed in a water treatment machine. The water pressure was controlled at from 1 bar to 7 bar. The polymer films subjected to water pressure were placed in a petri dish and dried in a vacuum dryer for at least three days. The dried surface of membrane was confirmed using a scanning electron microscope (SEM), and the change of functional groups before and after water treatment was observed by Fourier transform-infrared (FT-IR). Thermal decomposition temperature of the membrane was confirmed by thermogravimetric analysis (TGA).

It was possible to observe the state of pores for the membrane through SEM under a voltage of 30 kV (JSM-5600LV, JEOL). The interaction of the functional group, such as ether group and carbonyl group between the plasticizer lactic acid (LA) and the polymer CP, was confirmed through FT-IR at 32 scans and resolution 4 cm<sup>-1</sup> (VERTEX 70/70V FT-IR spectrometers, Bruker optics). TGA was measured for thermal decomposition (Universal V4. 5A, TA instruments).

## RESULTS AND DISCUSSION

The size of pores and shape between pores were observed by SEM. Fig. 1(a) is the surface of the neat CP dissolved in DMAc/EtOH (8:2 wt%), and it shows the smooth surface without pores. Likewise, Fig. 1(b) to indicate the membrane CP containing lactic acid (1:0.05) dissolved in DMAc/EtOH (8:2), also has no pores on its surface. Contrastively, Fig. 1(c) to indicate the surface of the membrane, which was subjected to water-pressure treatment up to 7 bar with lactic acid, shows many pores throughout the membrane. Unlike Fig. 1(a) and Fig. 1(b), many pores were generated only in Fig. 1(c) since the membrane was plasticized and became flexible by the additive LA, and the pores were pierced by the water pressure treatment. Fig. 1(d) shows the cross-section of CP with LA (1:0.05) dissolved in DMAc/EtOH (8:2) at 7 bar.

FT-IR was used to determine the interaction between cellulose propionate and lactic acid. The carbonyl group has a peak at around 1,750 cm<sup>-1</sup>, and the ether group has a peak at 1,060 cm<sup>-1</sup>. Fig. 2 shows the change of the wavenumber of each functional group from neat CP membrane treated by 0 bar and 7 bar. Since there was no remarkable change in wavenumber in FT-IR, deconvolution was carried out to obtain the accurate values. The value of FT-IR can be observed in more detail through deconvolution. Fig. 3(a), Fig. 3(b), and Fig. 3(c) show the deconvolution data of neat CP, CP:LA (1:0.05) at 0 bar and CP:LA (1:0.05) at 7 bar, respectively. As shown in the wavenumber of 1,724-1,729 cm<sup>-1</sup>, it indicates that the area becomes smaller at Fig. 3(c) than in Fig. 3(a). The wave-

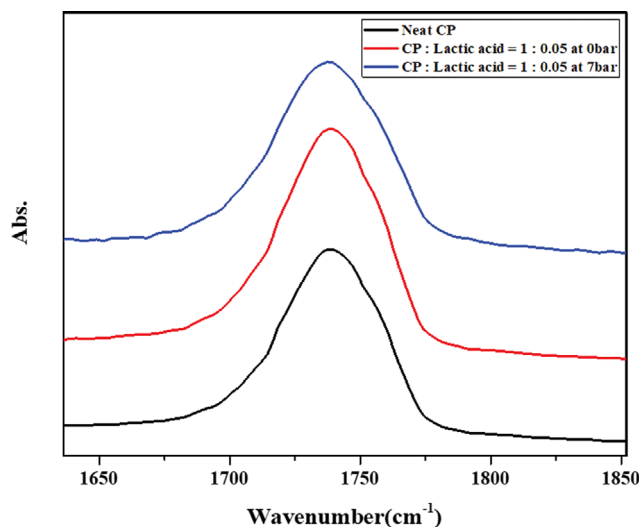


Fig. 2. FT-IR data of carbonyl groups: neat CP, 1:0.05 CP:lactic acid (0 bar), and 1:0.05 CP:lactic acid (7 bar).

Table 1. Deconvolution data of each functional group in IR analysis

Wavenumber	Neat CP	CP/LA at 0 bar	CP/LA at 8 bar
1,724-1,729 cm <sup>-1</sup>	43.22%	37.75%	32.97%
1,738-1,740 cm <sup>-1</sup>	52.14%	58.80%	63.38%
1,759-1,760 cm <sup>-1</sup>	4.64%	3.45%	3.65%

number of 1,738-1,740 cm<sup>-1</sup> becomes the dominant peak with the largest area (Table 1), and it shows that the area increases as LA is added and water pressure is treated. This is attributable to the fact that when LA was penetrating into between chains, the membrane became plasticized and pores were generated, inducing the change of distance in chains. Subsequently, when water pressure was applied, the interaction decreased as the distance between the carbonyl groups in the chain increased, and the vibration became stronger only within a single carbonyl group.

FT-IR analysis showed that the ether group did not interact with lactic acid, judging from that the value in Fig. 2 was not changed. Furthermore, the dominant peak shifted to the left when lactic acid was added. The interaction between LA and CP weakened the bond of carbonyl group and moved to a lower wavenumber. It indicates that the membrane was plasticized due to LA. However, the main peak became recovered when the water pressure treatment was performed up to 7 bar, presuming that LA was removed after the water pressure treatment. Thus, it could be thought that the interaction between LA and CP is reduced, but a small amount of LA remained.

TGA was used to determine the thermal decomposition temperature of the CP and CP/lactic acid composites. Fig. 4(a) shows TGA data of neat CP, CP:LA (1:0.05 mol ratio) at 0 bar and CP:LA (1:0.05 mol ratio) at 7 bar. Fig. 4(b) is an enlarged part of the temperature at which thermal decomposition occurred. As shown at Fig. 4(b), the fabricated membrane undergoes thermal decomposition between 300 and 350 °C. The membrane that the plasticizer LA was added and was not subjected to water pressure treatment

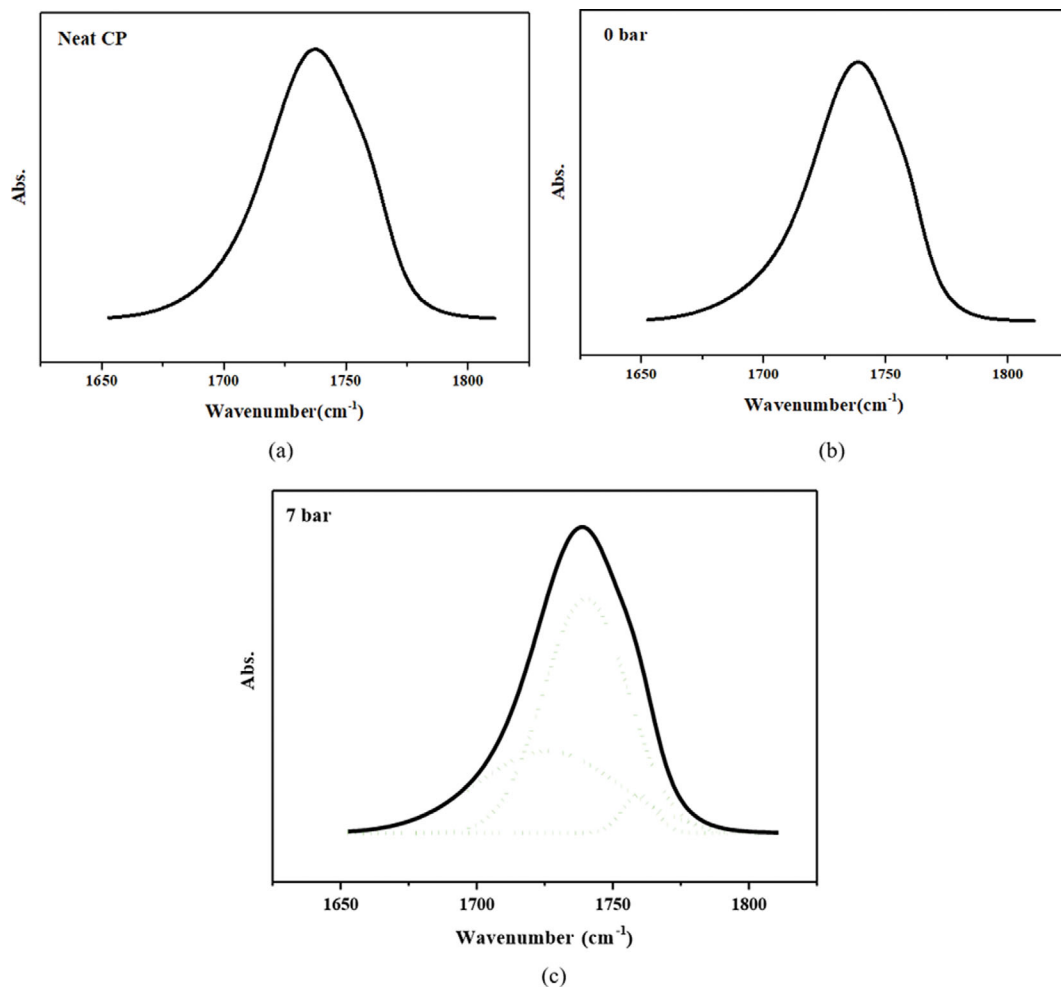


Fig. 3. FT-IR of deconvolution data of (a) neat CP (b) CP:LA (1:0.05) at 0 bar and (c) CP:LA (1:0.05) at 7 bar.

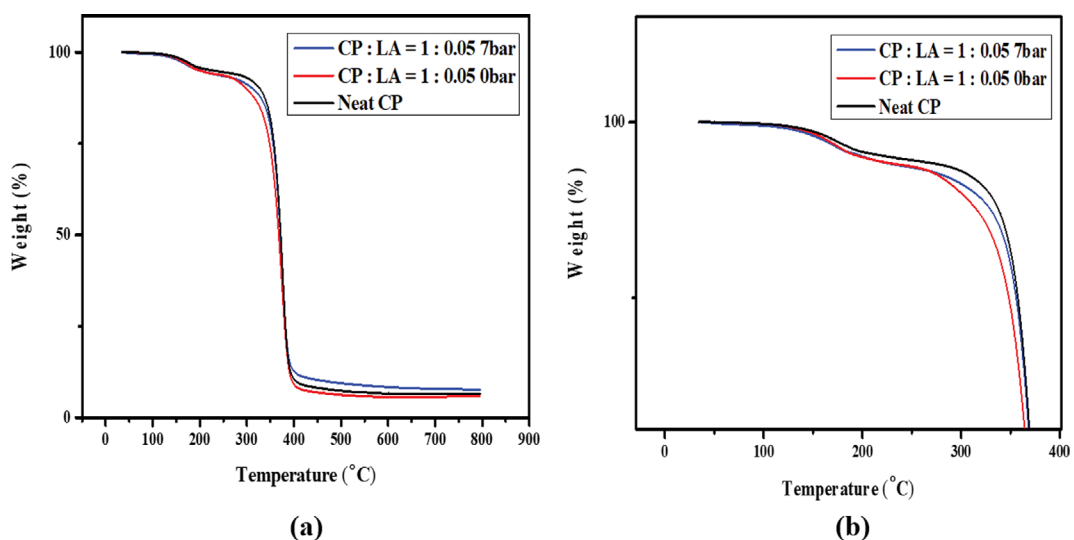


Fig. 4. TGA data of (a) neat CP and 1:0.05 mol ratio of CP:LA membrane at 0 and 7 bar (b) enlargement of (a).

shows the fastest thermal decomposition. Since the CP membrane containing additive LA was plasticized, the temperature at which it was collapsed is lower than that of the neat CP membrane. The

reason why the film containing the plasticizer was thermally decomposed faster is that the mechanical strength became weaker as the film became flexible. However, the temperature at which the neat

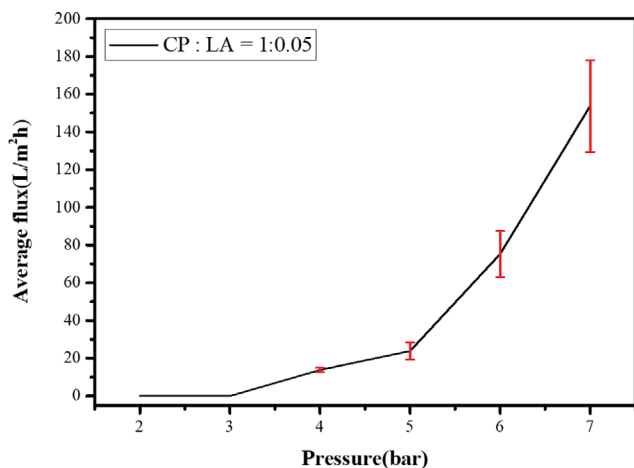


Fig. 5. Water flux data of the 1 : 0.05 CP : LA membrane from 2 to 7 bar.

CP membrane collapsed is similar to that of the membrane subjected to water pressure treatment up to 7 bar, even though the membrane is plasticized by LA to generate the pores. This shows that the manufactured membrane was restored for thermal stability. It is thought that the plasticizer LA escaped through water treatment and the structure created by the pores in the membrane makes the mechanical strength stronger.

Water flux is a value to represent the transport amount through the area of the membrane per time, and the unit is L/m<sup>2</sup>h (LMH). From the result values of water flux, it can be seen that pores through which the material can pass were formed. The water pressure was raised from 2 to 7 bar through a water treatment machine. As a result, as the pressure increased, the water flux value increased as shown in Fig. 5. On average, 13.809 LMH at 4 bar, 23.799 LMH at 5 bar, 75.280 LMH at 6 bar, and 153.745 LMH at 7 bar were measured, and extremely increased after 7 bar, while the water flux was not observed for neat CP polymer. This water flux data shows that the higher the water pressure, the more pores formed in the CP polymer and the faster the material moves. Compared to the water flux value of the membrane using the same plasticizer LA for the cellulose acetate (CA), the results show that the water flux value of the membrane made of CP is higher than that of CA, indicating that pores are well generated in the polymer prepared in this experiment. Compared to the experiments using CA with other additives, the higher value of water flux in this experiment indicates that porosity control is easier when LA is added as a plasticizer.

## CONCLUSION

We have researched for creating pores in a separator using cellulose acetate. Since CA has a low molecular weight, it requires a support to increase mechanical strength. In this study, a separator was prepared from a single film using cellulose propionate to have a higher mechanical strength than CA without additional support. When manufacturing a separator of a battery, it is desirable to generate pores in straight lines as much as possible in the membrane since it is efficient when the movement path of ions is minimized.

LA was used as an additive to solvate the polymer chains for partial plasticization. Through SEM analysis, the shape of pores formed in the membrane due to water treatment was observed. When investigating the thermal decomposition temperature by TGA analysis, the addition of plasticizer LA induced it to be more flexible, and polymer was collapsed at a lower temperature. After water treatment, the thermal decomposition temperature seemed to be recovered to its initial state, but LA was not completely removed from polymer chains. However, if LA was not removed completely, electrolyte wettability would be improved, which can be an advantage when charging a battery. FT-IR analysis was conducted to observe changes in the functional groups of LA and CP. With the addition of LA, the binding strength of the C=O bond became weaker. When LA was added, the carbonyl group peak became weakened due to the interaction with CP, and the main peak moved to a lower wavenumber, indicating the plasticization generated by LA.

## AUTHORS' CONTRIBUTIONS

- J. Lee collected the data and wrote the draft.
- S. W. Kang analyzed the data and reviewed the draft.

### Data availability: not applicable

**Funding:** This research was funded by a 2022 Research Grant from Sangmyung University (2022-A000-0053).

### Conflicts of interests/Competing interests: not applicable

## REFERENCES

1. B. Frieske, M. Kloetzke and F. Mauser, Trends in vehicle concept and key technology development for hybrid and battery electric vehicles. 2013 world electric vehicle symposium and exhibition (EVS27); IEEE (2013).
2. S. Hemavathi and A. Shinisha, *J. Energy Storage*, **52**, 105013 (2022).
3. J. A. Sanguesa, V. Torres-Sanz, P. Garrido, F.J. Martinez and J. M. Marquez-Barja, *Smart Cities*, **4**(1), 372 (2021).
4. R. Hemmati and H. Saboori, *Renew. Sust. Energy Rev.*, **65**, 11 (2016).
5. M. A. Hannan, M. M. Hoque, A. Mohamed and A. Ayob, *Renew. Sust. Energy Rev.*, **69**, 771 (2017).
6. D. Jahani, A. Nazari and M. Y. Panah, *Korean J. Chem. Eng.*, **39**, 2099 (2022).
7. Y. K. Park, S. C. Jung and H. Y. Jung, *Korean J. Chem. Eng.*, **40**, 91 (2023).
8. D. V. Pelegov, J. Pontes, *Batteries*, **4**(4), 65 (2018).
9. Y. Yang, E. G. Okonkwo, G. Huang, S. Xu, W. Sun and Y. He, *Energy Stor. Mater.*, **36**, 186 (2021).
10. Y. Liang, C. Zhao, H. Yuan, Y. Chen, W. Zhang and J. Huang, *Info-Mat.*, **1**(1), 6 (2019).
11. S. Saxena, G. Sanchez and M. Pecht, *IEEE Ind. Electron. Mag.*, **11**(2), 35 (2017).
12. Q. Wang, P. Ping, X. Zhao, G. Chu, J. Sun and C. Chen, *J. Power Sources*, **208**, 210 (2012).
13. D. Guo, L. Sun, X. Zhang, P. Xiao, Y. Liu and F. Tao, The causes of fire and explosion of lithium ion battery for energy storage. 2nd IEEE Conference on Energy Internet and Energy System Integra-

- tion (E12); IEEE (2018).
14. X. Huang, *J. Solid State Electrochem.*, **15**(4), 649 (2011).
  15. S. S. Zhang, *J. Power Sources*, **164**(1), 351 (2007).
  16. C. Kim, J. Yoo, K. Jeong, K. Kim and C. Yi, *J. Power Sources*, **289**, 41 (2015).
  17. X. Zhang, J. Zhu and E. Sahraei, *Rsc Adv*, **7**(88), 56099 (2017).
  18. P. Apel, *Radiat Measur.*, **34**(1-6), 559 (2001).
  19. G. S. Alkan, L. Gubler, B. Gupta and G. G. Scherer, *Fuel Cells*, **I**, 157 (2008).
  20. H. Bae and Y. Kim, *Mater. Adv.*, **2**(10), 3234 (2021).
  21. O. E. Bankole, C. Gong and L. Lei, *J. Environ. Ecol.*, **10**, 14 (2013).
  22. S. H. Kim and S. W. Kang, *Cellulose*, **28**(15), 10055 (2021).
  23. S. H. Kim and S. W. Kang, *Chem. Commun.*, **57**(71), 8965 (2021).
  24. S. H. Kim, Y. R. Choi, Y. J. Cho, S. Y. Rhyu and S. W. Kang, *Korean J. Chem. Eng.*, **38**, 1715 (2021).
  25. H. J. Lee and S. W. Kang, *Chem. Commun.*, **57**(36), 4388 (2021).
  26. H. J. Lee, Y. Cho and S. W. Kang, *J. Ind. Eng. Chem.*, **94**, 419 (2021).
  27. S. H. Hong, Y. Cho and S. W. Kang, *J. Ind. Eng. Chem.*, **91**, 79 (2020).